Available online at www.sciencedirect.com
SCIENCE DIRECT®
Journal of Solid State Chemistry 177 (2004) 3086–3091
JOURNAL OF SOLID STATE CHEMISTRY
http://elsevier.com/locate/jssc

Synthesis, crystal structure and magnetic properties of an Os-containing pillared perovskite $La_5Os_3MnO_{16}$

Lisheng Chi,[a] I.P. Swainson,[b] and J.E. Greedan[a,*]

[a] *Department of Chemistry & Brockhouse, Institute for Materials Research, McMaster University, Hamilton, Ontario, Canada L8S 4M1*
[b] *Neutron Program for Materials Research, NRC, Chalk River, Ontario, Canada K0J 1J0*

Received 15 March 2004; received in revised form 30 April 2004; accepted 6 May 2004

Available online 24 June 2004

Abstract

A new Os-containing, pillared perovskite, $La_5Os_3MnO_{16}$, has been synthesized by solid state reaction in sealed quartz tubes. This extends the crystal chemistry of these materials which had been known only for Mo and Re, previously. The crystal structure has been characterized by X-ray and neutron powder diffraction and is described in space group C-1 with parameters $a = 7.9648(9)$ Å; $b = 8.062(1)$ Å; $c = 10.156(2)$ Å, $\alpha = 90.25(1)^\circ$, $\beta = 95.5(1)^\circ$; $\gamma = 89.95(2)^\circ$, for $La_5Os_3MnO_{16}$. The compound is isostructural with the corresponding $La_5Re_3MnO_{16}$ phase. A very short Os–Os distance of 2.50(1) Å was found in the dimeric pillaring unit, Os_2O_{10}, suggestive of a triple bond as demanded by electron counting. Nearly spin only values for the effective moment for Os^{5+} ($S = \frac{3}{2}$) and Mn^{2+} ($S = \frac{5}{2}$) were derived from magnetic susceptibility data. Evidence for magnetic transitions was seen near ~180 and 80 K. Neutron diffraction data indicate that T_c is 170(5) K. The magnetic structure of $La_5Os_3MnO_{16}$ at 7 K was solved revealing that Os^{5+} and Mn^{2+} form ferrimagnetically coupled layers with antiferromagnetic interlayer ordering. The ordered moments are 4.2(4) μ_B for Mn^{2+} and 1.5(4) μ_B for Os^{5+}, which are reduced from the respective spin only values of 5.0 and 3.0 μ_B. The observation of net ferrimagnetic (antiparallel) intraplanar coupling between $Os^{5+}(t_{2g}^3)$ and $Mn^{2+}(t_{2g}^3e_g^2)$ is interesting as it appears to contradict the Goodenough-Kanamori rules for 180° superexchange.

Keywords: Os oxide; Pillared perovskites; Crystal and magnetic structure from neutron diffraction; Short range ferrimagnetism; Metamagnetism; Triple bonded Os dimeric unit

1. Introduction

Recently, new oxide materials containing transition elements from the 3*d*, 4*d*, 5*d* and 4*f* series in the same structure have been reported. These are the so-called "pillared" perovskites of composition $Ln_5M_3M'O_{16}$ in which corner sharing octahedral layers, $MM'O_6$, with M, M' site ordering, are pillared by diamagnetic edge-sharing octahedral dimeric units, M_2O_{10}, as seen in Fig. 1, where the Ln^{3+} ions occupy interstitial sites. The dimeric pillaring units involve multiple M–M bonds. To date this structure type has been found for M = Mo or Re and M' = Mn, Fe, Co, Ni, Mg [1–6]. Due to the site ordering in the $MM'O_6$ layers which separates the 4*d* and 5*d* ions with O–M'–O "spacer" units, both the 4*d* or 5*d* element exhibit local moment behavior with effective magnetic moments near the spin only values. Within the layers ferrimagnetic short range spin correlations are seen as illustrated in Fig. 2 for the $La_5Re_3CoO_{16}$ material. χT shows an initial decrease from the observed Curie constant upon cooling due to the antiparallel nature of the coupling between Co^{2+} ($S = \frac{3}{2}$) and Re^{5+} ($S = 1$). As the correlation length of the ferrimagnetic clusters grows, one sees the influence of the net cluster moment in a rapid increase in χT as the phase transition is approached from above. In other cases, perhaps surprisingly, given the >10 Å interplanar separation, long range magnetic order is found at relatively high temperatures, for example ~200 K for $La_5Mo_4O_{16}$ and 162 K for $La_5Re_3MnO_{16}$ [2,3]. In the materials studied in detail so far, namely $La_5Re_3MnO_{16}$ and $La_5Re_3FeO_{16}$, the long range order observed involves antiferromagnetic coupling of the ferrimagnetic

*Corresponding author.
E-mail address: greedan@mcmaster.ca (J.E. Greedan).

0022-4596/$ - see front matter © 2004 Elsevier Inc. All rights reserved.
doi:10.1016/j.jssc.2004.05.014

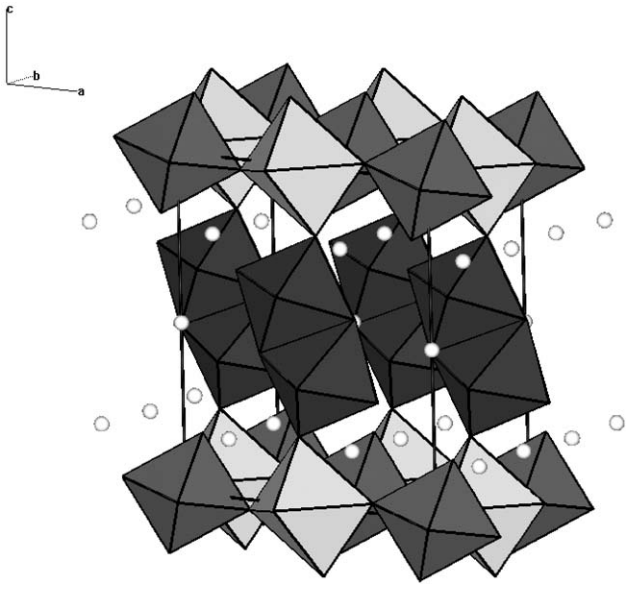

Fig. 1. Crystal structure of a "pillared" perovskite. Note the corner-sharing octahedral layers, pillared by edge-sharing dimers. For $La_5Os_3MnO_{16}$, the gray and white octahedra in the layers represent Os and Mn, respectively, the dimers are shown in black and the white spheres represent the La^{3+} sites. Note that the interlayer connection via the dimers is through the Mn-centered octahedra.

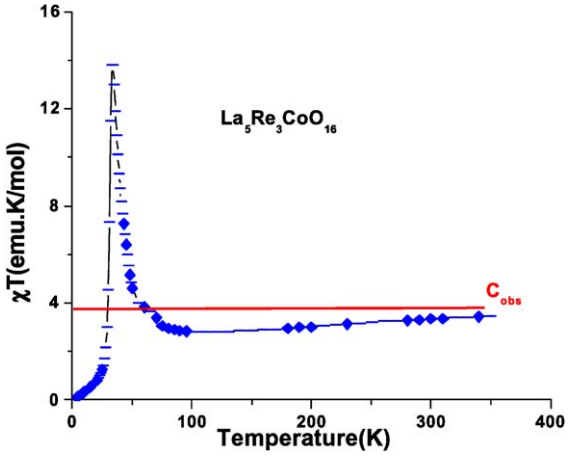

Fig. 2. Evidence for ferrimagnetic short range correlations in the pillared perovskite, $La_5Re_3CoO_{16}$.

layers [4,5]. It is of interest to extend the crystal chemistry of this class of oxides to include other elements. In this study the successful preparation of $La_5Os_3MnO_{16}$ and its partial characterization is described. Os^{5+} has one more electron than Re^{5+} and thus, $S = \frac{3}{2}$ rather than $S = 1$ and systematic changes in magnetic properties are expected. As well, the dimeric Os_2O_{10} unit should involve an Os≡Os triple bond.

2. Experimental

2.1. Synthesis

$La_5Os_3MO_{16}$ (M = Mn, Co) was synthesized from La_2O_3 (99.9%, Aldrich), OsO_2 (99.9%, Aldrich), MnO (99.99%, Aldrich). La_2O_3 was dried at 800°C overnight before use. Stoichiometric chemicals were accurately weighed according to the following equation:

$$5La_2O_3 + 6OsO_2 + 2MnO + \tfrac{3}{2}O_2 \rightarrow 2La_5Os_3MnO_{16}$$

0.5 gram of the mixture was ground, pressed into a pellet, loaded in a platinum crucible and sealed under high vacuum ($\geqslant 10^{-6}$ mmHg) in a quartz tube along with a pellet of $KClO_3$, as the oxygen source, wrapped in platinum foil. *It was common practice to seal the quartz tube containing the reactants in a larger diameter quartz tube as a precaution against its possible rupture due to the decomposition of $KClO_3$. This is strongly recommended.* The pellet was centred in a tubular furnace and heated to 1000°C in 24 h, and held for another 24 h for solid state reaction. Oxygen was liberated by decomposition of $KClO_3$ upon heating. A black powder was obtained.

2.2. X-ray and neutron diffraction

The purity of polycrystalline product was examined using a Guinier camera with Cu$K\alpha_1$ radiation $\lambda = 1.54056$ Å and high-purity silicon powder as an internal standard. X-ray diffraction data used for Rietveld refinement were collected on a Bruker D8 diffractometer using Cu$K\alpha_1$ radiation in the range of $10° \leqslant 2\theta \leqslant 80°$. A 2θ step size of 0.02° and a step time of 10 s were used. Neutron diffraction data collection was carried out on $La_5Os_3MnO_{16}$ using the $C2$ diffractometer, which is operated by the Neutron Program for Materials Research of the National Research Council of Canada at the AECL Chalk River Laboratories. The data were collected in the angular ranges of $5° \leqslant 2\theta \leqslant 116.9°$ at room temperature (298 K) with wavelength 1.32671 Å, and $3° \leqslant 2\theta \leqslant 109.9°$ at several temperatures below 210 K with wavelength 2.36877 Å and the same step interval of 0.1°.

2.3. Magnetic properties

Magnetic data collection was performed on a SQUID magnetometer (Quantum Design MPMS). The temperature dependence of the magnetic susceptibility with both ZFC/FC (zero field cooled and field cooled) modes was obtained for $La_5Os_3MnO_{16}$ in a temperature range of 2–350 K and an isothermal magnetization measurement was done using applied fields of 0–5.5 T. An oven insert was used to collect high temperature (300–600 K) susceptibility data. The molar magnetic susceptibility data presented in this paper all were corrected for the diamagnetic contributions of the constituent atoms.

3. Results and discussion

3.1. X-ray and neutron characterization

The Guinier powder pattern for $La_5Os_3MnO_{16}$ is similar to the Re-containing materials in this family except for weak peaks at $2\theta = 20.30°$, 28.83°, 30.73°, 31.35°, 33.79° and 43.80° due to an unidentified impurity phase. Rietveld analysis of the powder neutron data was carried out with $La_5Re_3FeO_{16}$ as a initial model using the FULLPROF program [7] and excluding regions effected by the impurity phase (the intensities of the impurity peaks were $<5\%$ of the strongest structure peaks), yielding agreement factors $R_p = 2.48$, $R_{wp} = 3.23$, $\chi^2 = 12.7$, $R_B = 7.55$. The high value for χ^2 is due to the relatively high background, all other indices are acceptable. In the Rietveld analysis, the background levels were fitted by Chebyshev polynominals, and the peak shapes were described by pseudo-Voigt functions. The observed, calculated and difference diffraction profiles are presented in Fig. 3. The final atomic coordinates and thermal parameters are displayed in Table 1 and the selected bond distances and bond angles are listed in Table 2.

As shown in Fig. 1, the crystal structure of $La_5Os_3MnO_{16}$ is isostructural with the Re-based compounds. MnO_6(white) and OsO_6(gray) octahedra are linked through corners to form magnetic perovskite layers which are pillared by dimeric Os_2O_{10} units(black), within which OsO_6 octahedra share a common edge with an Os–Os distance of 2.50(1) Å. A bond valence calculation shows that the oxidation state of Os1 is +5.1. As Os_2^{10+} is a $d3-d3$ electronic system, an Os≡Os triple bond with a σ bond and two π bonds is expected to form within the dimer. Similar Os–Os distances characteristic of Os≡Os triple bonds have been found in $La_3Os_2O_{10}$ [2.468(1) Å] [8], $La_4Os_6O_{19}$ [2.499(1) Å] [9] and $Os(DFM)_4Cl_2$ [2.4672(6) Å] [10]. Another important structural feature is the intraplanar Os–O–Mn bond angle. In fact there are two such angles at 153° and 146°, much reduced from the 180° for an ideal perovskite layer and this will play a role in determining the intraplanar magnetic properties.

3.2. Magnetism

Fig. 4 presents the molar magnetic susceptibility of $La_5Os_3MnO_{16}$ as a function of temperature with both zero field-cooling (ZFC) and field cooling (FC) modes. At high temperatures, the ZFC and FC curves are indistinguishable and reach a rather broad maximum near ~178 K below which the curves separate. The ZFC curve shows a second, much more pronounced, maximum near 78 K. The Curie–Weiss regime is not found until rather high temperatures, between 510 and 600 K (see inset). Fitting of these data to $\chi = C/(T-\theta)$, where χ is the molar susceptibility, C is the Curie constant and θ is the Weiss temperature, yields $C = 6.06(4)$ (emu/mol K), comparable to the sum of values for Os^{5+}[d^3, $C = 1.87$ (emu/mol K)] and Mn^{2+}[d^5, $C = 4.38$ (emu/

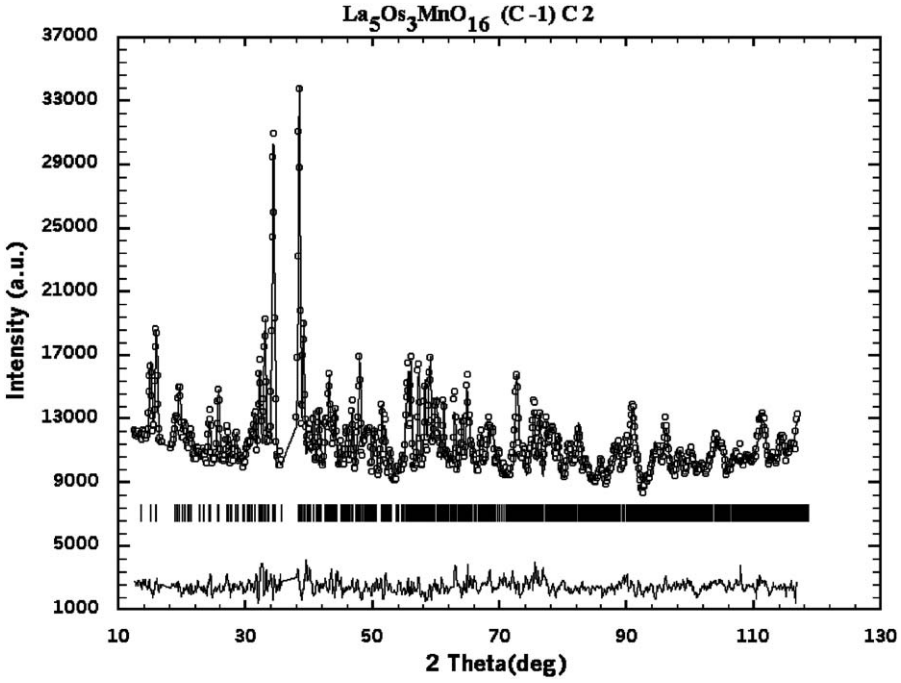

Fig. 3. Rietveld fit of neutron powder data for $La_5Os_3MnO_{16}$ at 298 K. The open circles are the data, the solid line is the fit, the lower line is the difference plot and the vertical tic marks locate the Bragg peaks.

Table 1
Atomic coordinates and displacement factors for $La_5Os_3MnO_{16}$

Name	x	y	z	B (Å^2)
La1	0.223(1)	0.740(1)	0.7936(9)	1.5(2)
La2	0.237(2)	0.271(2)	0.793(2)	2.6(4)
La3	0.50000	0.50000	0.50000	1.57(3)
Os1	0.057(1)	0.497(1)	0.3893(9)	0.8(2)
Os2	0.00000	0.00000	0.00000	0.3(2)
Mn	0.00000	0.50000	0.00000	1.7(8)
O1	0.184(2)	0.520(3)	0.579(1)	0.4(2)
O2	0.274(2)	0.498(3)	0.322(1)	0.6(3)
O3	−0.039(2)	0.500(3)	0.197(1)	0.02(25)
O4	0.074(3)	−0.019(3)	0.181(2)	2.27(4)
O5	0.036(2)	0.738(2)	0.364(1)	1.21(5)
O6	0.053(4)	0.264(3)	0.382(2)	2.7(6)
O7	−0.060(2)	0.242(3)	0.006(2)	1.1(2)
O8	0.241(3)	0.051(2)	−0.046(2)	0.7(3)

Note: $a = 7.9604(9)$ Å, $b = 8.056(1)$ Å, $c = 10.148(1)$ Å, $\alpha = 90.25(1)^\circ$, $\beta = 95.49(1)^\circ$, $\gamma = 89.94(1)^\circ$.

Table 2
Selected bond distances (Å) and angles (deg) for $La_5Os_3MnO_{16}$

Bond distances		Bond angles	
Os1–Os1	2.504(13)	O(4)–Os(2)–O(7)	97(2)
Os1–O1	2.095(17)	O(4)–Os(2)–O(7)	83(2)
Os1–O1	1.984(19)	O(4)–Os(2)–O(8)	91(2)
Os1–O2	1.916(19)	O(4)–Os(2)–O(8)	89(2)
Os1–O3	2.029(18)	O(7)–Os(2)–O(8)	91(2)
Os1–O5	1.970(20)	O(7)–Os(2)–O(8)	89(2)
Os1–O6	1.874(32)	O(3)–Mn–O(7)	83(2)
Os2–O4	1.879(21) × 2	O(3)–Mn–O(7)	97(2)
Os2–O7	2.011(22) × 2	O(3)–Mn–O(8)	88(1)
Os2–O8	2.060(21) × 2	O(3)–Mn–O(8)	92(2)
Mn–O3	2.050(15) × 2	O(7)–Mn–O(8)	89(2)
Mn–O7	2.134(22) × 2	O(7)–Mn–O(8)	91(2)
Mn–O8	2.113(21) × 2	Os(2)–O(7)–Mn	152.6(95)
		Os(2)–O(8)–Mn	145.5(9)

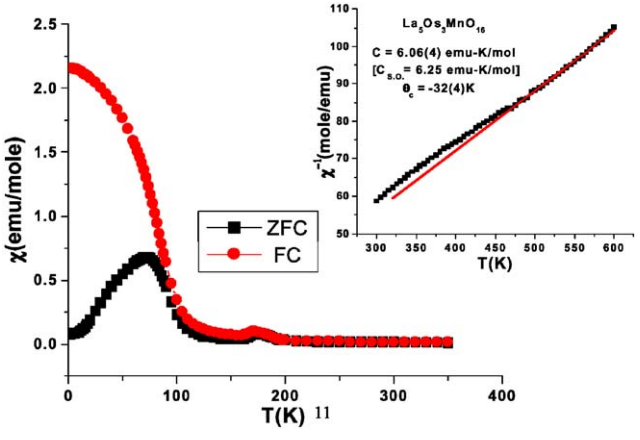

Fig. 4. The molar magnetic susceptibility of $La_5Os_3MnO_{16}$ as a function of temperature carried out at an applied field of 500 Oe in ZFC (zero field cooling) and FC (field cooling) modes. Two transition temperatures occur at ~78 and ~178 K. The inset is inverse susceptibility up to 600 K and the fitted line indicates a Curie–Weiss law above 510 K.

mol K)] and $\theta = -32(4)$ K. The close agreement of the observed Curie constant with the spin-only values for the two ions involved, indicates local moment behavior. Although the Weiss constant is negative, it is slightly less negative than that for $La_5Re_3MnO_{16}$ which is −48 K. This result is somewhat surprising as the $(t_{2g}^3 e_g^2 - t_{2g}^3)$ interaction is predicted to be strongly ferromagnetic according to the Goodenough-Kanamori rules for 180° superexchange [11,12]. It is possible that a ferromagnetic nearest neighbor exchange is weakened by the decrease in Os–O–Mn angle to 153° and 146° from the ideal 180° and is dominated, ultimately, by farther neighbor interactions and the interplanar exchange which must be weak but is antiferromagnetic.

The magnetization as a function of applied magnetic field at different temperatures is shown in Fig. 5. A linear dependence is seen at 250 K, consistent with paramagnetism, while a weak curvature sets in at 170 K, just near the first phase transition. Evidence for a field-induced transition is apparent for $T = 130$ and 60 K at 2.5 T while this appears to be quenched at 5 K (although there is a hint of an upturn at ~5 T). The origin of this field-induced transition can be ascribed to the destruction of the interlayer AF coupling. The intralayer correlations are actually ferrimagnetic and presumably quite strong, while the relatively weak interlayer antiferromagnetic correlations can be overcome by applied fields in the laboratory range. Thus, the saturation moment expected is that for the ferrimagnetic layer which is $2\,\mu_B$ for the $Os^{5+}(S = \frac{3}{2})$–$Mn^{2+}(S = \frac{5}{2})$ combination and spin-only moments. While saturation is not reached at any temperature here, the magnetization values are consistent with an approach to $2\,\mu_B$. Note that for ferromagnetic intraplanar coupling a saturation moment of $8\,\mu_B$ would be expected which is simply not supported by the data of Fig. 5. This isothermal magnetization behavior parallels that found in the $La_5Re_3MO_{16}$ (M = Mn, Fe, Co, Ni) series but for

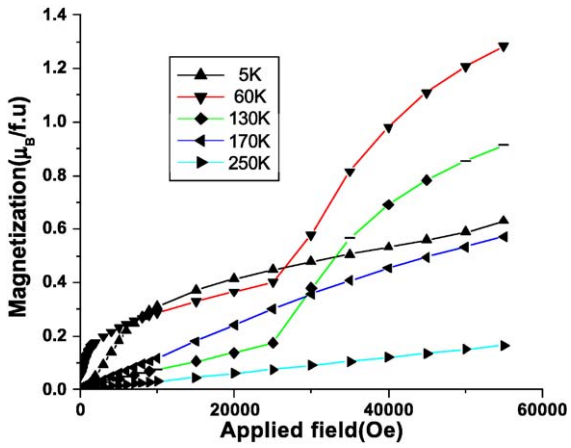

Fig. 5. Isothermal magnetization—field sweeps for selected temperatures.

which the transition critical fields are much lower, <0.5 T for intermediate temperatures and 1.5 T for 5 K which points to significantly stronger interlayer coupling for the Os—based material. In the absence of information on magnetocrystalline anisotropy in these compounds, which can only be obtained from single crystal studies, it is not clear whether the field-induced transitions are of the meta-magnetic (anisotropy dominated) or the spin-flop (exchange dominated) type although the discussion above implies the latter. For the two ions involved, $Os^{5+}(5d^3)$ and $Mn^{2+}(3d^5)$, one expects fairly well quenched orbital contributions in a quasi-octahedral environment and, therefore, that magnetocrystalline anisotropy should be less important than exchange but there are no actual data to support this plausible assumption.

4. Magnetic neutron diffraction

Low angle powder neutron diffraction patterns at selected temperatures are plotted in Fig. 6, showing four well-resolved magnetic reflections, which develop with decreasing temperature. These can be indexed on a magnetic unit cell with $a_{mag} = a$, $b_{mag} = b$, $c_{mag} = 2c$, i.e., with an ordering wave vector $\mathbf{k} = (0,0,\frac{1}{2})$. The intensities of the $(11\frac{1}{2})$ and $(-11\frac{1}{2})$ reflections, the two strongest magnetic features, are plotted as a function of temperature in Fig. 7, showing consistency with $T_c = 170(5)$ K, in reasonable agreement with the bulk magnetic data. Note that no obvious change in intensity occurs near the lower temperature peak, ~ 78 K in the bulk susceptibility, suggesting that this feature may arise from a more subtle effect, perhaps a spin re-orientation.

The magnetic structure of $La_5Os_3MnO_{16}$ was refined from a 7 K data set obtained using $\lambda = 2.36877$ Å neutrons. All profile and atomic parameters were refined with the exception that displacement factors for each type of atom, La, Os, Mn and O were constrained to be equal. The starting model for the magnetic structure was

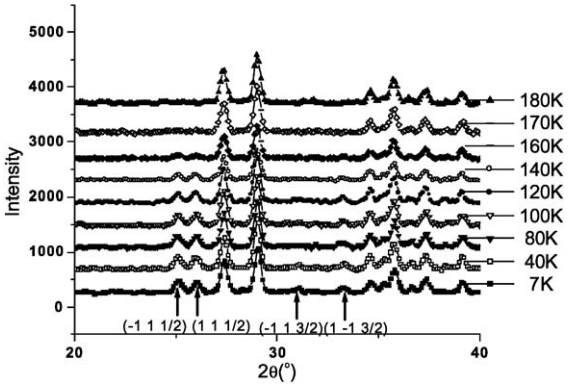

Fig. 6. Low angle neutron powder diffraction data ($\lambda = 2.36877$ Å) showing the temperature dependence of magnetic reflections.

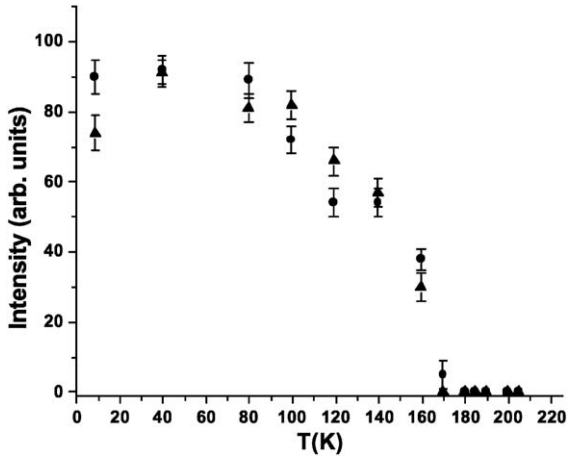

Fig. 7. The temperature dependence of the intensity of the $(-11\frac{1}{2})$ ■ and $(11\frac{1}{2})$ ▲ reflections showing $T_c = 170(5)$ K.

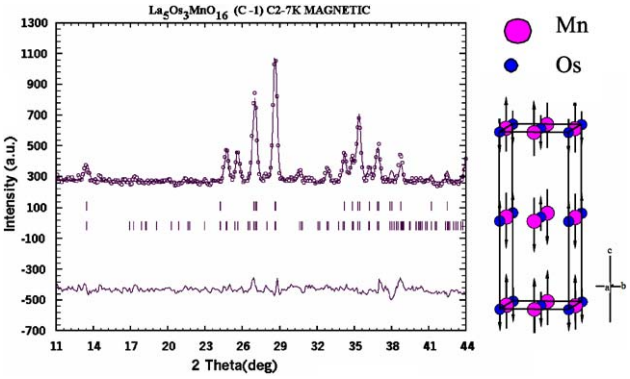

Fig. 8. (Left hand side) Rietveld analysis of the low angle region showing the excellent fit of the model to the strongest magnetic reflections. (Right hand side) The proposed model for the magnetic structure of $La_5Os_3MnO_{16}$.

that of $La_5Re_3FeO_{16}$ [5]. The Mn^{2+} and Os^{5+} moments refined to $\mu_{Mn^{2+}} = 4.2(4)\,\mu_B$ and $\mu_{Os^{5+}} = 1.5(4)\,\mu_B$, with both parallel to the c-axis. There is no evidence for magnetic reflections of the type (00l), which re-enforces the moment orientation along c. Reasonable agreement is found with the expected spin only value for $Mn^{2+}(5.0\,\mu_B)$ but the Os^{5+} moment is significantly lower than $3.0\,\mu_B$. The resulting magnetic structure is shown in Fig. 8 along with the low angle part of the Rietveld refinement, showing the excellent fit to the four most intense magnetic peaks. The agreement indices for this refinement are $R_p = 5.82$. $R_{wp} = 7.66$, $\chi^2 = 2.39$, $R_B = 8.95$ and $R_{MAG} = 24.5$. While the R_{MAG} value appears to be large, it is similar to that reported for the corresponding $La_5Re_3MnO_{16}$ magnetic structure, 22.7 [4]. In fact if only the low angle magnetic reflections, $2\theta < 40°$, are used, $R_{MAG} = 13.5$. The observation of net ferrimagnetic intraplanar coupling between Os^{5+} and Mn^{2+} is consistent with the observed negative value for θ_c and the apparent saturation magnetization values from isothermal field sweep data.

5. Summary and conclusions

The chemistry of the pillared perovskite materials is extended to include Os with the preparation of $La_5Os_3MnO_{16}$. This compound is isostructural with $La_5Re_3MnO_{16}$. An Os≡Os triple bond within the pillaring Os_2O_{10} unit is indicated by a short, 2.50(1) Å, interdimer Os–Os distance. The magnetic properties are consistent with short range ferrimagnetic correlations within the perovskite-like $MnOsO_6$ layers and long range overall antiferromagnetic order below $T_c = 170$ K involving the coupling of the ferrimagnetic layers. This is slightly higher than $T_c = 161$ K for $La_5Re_3MnO_{16}$ which could be attributed in part to the slightly shorter *c*-axis length for the Os phase (10.156 Å) relative to the Re phase (10.227 Å). Field-induced transitions occur at ~ 2.5 T for temperatures below T_c. These are significantly larger critical fields than those observed in the isostructural $La_5Re_3MnO_{16}$ compound, indicative of stronger interplanar coupling in the Os-based material. The magnetic structure is the same as that for $La_5Re_3FeO_6$ with an ordered moment on Mn^{2+} near the spin-only value but a much reduced Os^{5+} moment. A possible violation of the Goodenough-Kanamori rules for the intraplanar magnetic coupling is noted and qualitative explanations are offered.

Acknowledgments

This work was financially supported by the Natural Science and Engineering Research Council of Canada through a Research Grant to J.E.G.

References

[1] M. Ledesert, Ph. Labbe, W.H. McCarroll, H. Leligny, B. Raveau, J. Solid State Chem. 105 (1993) 143.
[2] K.V. Ramanuchary, M. Greenblatt, W.H. McCarroll, J.B. Goodenough, Mat. Res. Bull. 28 (1993) 1257.
[3] C.R. Wiebe, A. Gourrier, T. Langet, J.F. Britten, J.E. Greedan, J. Solid State Chem. 151 (2000) 31.
[4] A.E.C. Green, C.R. Wiebe, J.E. Greedan, Solid State Sci. 4 (2002) 305.
[5] L. Chi, A.E.C. Green, R. Hammond, C.R. Wiebe, J.E. Greedan, J. Solid State Chem. 170 (2003) 165–175.
[6] K.V. Ramanujchary, S.E. Lofland, W.H. McCarroll, T.J. Emge, M. Greenblatt, M. Croft, J. Solid State Chem. 164 (2002) 60.
[7] J. Rodriguez-Carvajal, FULLPROF, Version 3.5d, 1998.
[8] F. Abraham, J. Trehoux, D. Thomas, J. Solid State Chem. 29 (1979) 73.
[9] F. Abraham, J. Trehoux, D. Thomas, Mat. Res. Bull. 12 (1977) 43.
[10] F.A. Cotton, T. Ren, J. Eglin, Inorg. Chem. 30 (1991) 2559.
[11] J.B. Goodenough, Magnetism and the Chemical Bond, Wiley, New York, 1963.
[12] J. Kanamori, Phys. Chem. Solids 10 (1959) 87.